PTEN signaling through RAF1 proto-oncogene serine/threonine kinase (RAF1)/ERK in the epididymis is essential for male fertility

Bingfang Xu, Angela M. Washington, and Barry T. Hinton[1]

Department of Cell Biology, University of Virginia Health System, Charlottesville, VA 22908

Edited by John J. Eppig, The Jackson Laboratory, Bar Harbor, ME, and approved November 21, 2014 (received for review July 14, 2014)

Without a fully developed initial segment, the most proximal region of the epididymis, male infertility results. Therefore, it is important to understand the development and regulation of this crucial region. In addition to distinctively high activity levels of the components of the ERK pathway, which are essential for initial-segment differentiation, the initial segment exhibits high protein and activity levels of phosphatase and tensin homolog (PTEN). To understand the role of PTEN in the regulation of the initial segment, we generated a mouse model with a conditional deletion of *Pten* from the epithelial cells of the proximal epididymis from postnatal day 17 (P17) onward. Shortly after *Pten* deletion, hypertrophy of the proximal epididymis became evident. Loss of *Pten* resulted in activation of the AKT (protein kinase B) pathway components from P28 onward, which in turn gradually suppressed RAF1 proto-oncogene serine/threonine kinase (RAF1)/ERK signaling through the interaction between AKT and RAF1. Consistent with progressive changes in RAF1/ERK signaling, loss of *Pten* progressively altered cell shape, size, organization, proliferation, and survival in the initial-segment epithelium and resulted in dedifferentiation and extensive epithelial folding. Most importantly, knockout males progressively lost fertility and became infertile from 6 to 12 mo. Spermatozoa from older knockout mice showed a lower percentage of motility and a higher percentage of flagellar angulation compared with controls, suggesting compromised sperm maturation. Therefore, under normal physiological conditions, PTEN suppresses AKT activity to maintain activation of the RAF1/ERK signaling pathway, which in turn maintains normal function of the initial segment and therefore, normal sperm maturation.

epididymis | PTEN | RAF1/ERK signaling | male infertility | spermatozoa flagellar angulation

Spermatozoa enter the epididymis from the testes as immotile cells that are incapable of fertilization. During epididymal transit, a complex process called sperm maturation allows for conversion of spermatozoa into motile and fertilization-competent cells. The long, convoluted epididymal duct—which is ~6 m long in humans and 1 m in mice (1)—provides a luminal fluid microenvironment that is necessary for sperm maturation (2).

It is apparent that the most proximal region of the epididymis, the initial segment, plays an important role in sperm maturation. C-ros oncogene 1 (*Ros1*) knockout male mice that lacked prepubertal differentiation of the epididymal initial segment were healthy but infertile (3). Spermatozoa from *Ros1* knockouts showed flagellar angulation, a defect in sperm maturation (4). Therefore, it is important to examine the mechanisms by which the initial segment develops, functions normally, and contributes to normal sperm maturation.

The initial segment exhibits high activity levels of the ERK pathway components. The ERK pathway [also known as the RAF (RAF proto-oncogene serine/threonine kinases)/MEK/ERK pathway] is an intracellular protein kinase cascade containing at least MAPK3 and/or MAPK1 (commonly known as ERK1 and ERK2), a MAPKK (commonly known as MEK), and a MAP3K (including RAF1). The kinases in each tier phosphorylate and activate the kinases in the downstream tier to transmit a signal within a cell. During prepubertal development, the first wave of testicular luminal fluid enters the epididymis and activates the ERK pathway components in the initial-segment epithelium. The activated ERK pathway then promotes initial-segment differentiation (5), which is demonstrated by tall, columnar principal cells and long projections of basal cells (6, 7). Efferent duct ligation prevents luminal fluid from entering the epididymis and abolishes the high activity levels of the ERK pathway components in the initial segment (5, 8). Such abolishment results in the arrest of ongoing initial-segment differentiation in juvenile mice (5). Therefore, the high activity levels of the ERK pathway components are essential for differentiation of the initial-segment epithelium.

In addition to higher activity levels of the ERK pathway components, the initial segment exhibits higher protein and activity levels of phosphatase and tensin homolog (PTEN) compared with other epididymal regions (5). It is known that PTEN dephosphorylates PIP_3 and negatively regulates AKT (protein kinase B) activity. However, the significance of PTEN-regulated AKT signaling in the initial segment is unclear. To examine the role of PTEN in the initial segment, we generated a mouse model with a conditional deletion of *Pten* from epithelial cells of the proximal epididymis from postnatal day 17 (P17) onward. Results from our studies show that PTEN plays an essential role in maintaining normal initial-segment differentiation and function and, therefore, male fertility.

Results

Hypertrophy Phenotype in the Proximal Epididymis Shortly After Loss of *Pten*. *Rnase10*–Cre-mediated *Pten* deletion was initiated at P17 in the proximal epididymis. At P28, hypertrophy phenotype became

Significance

Without a fully developed and functioning initial segment, the most proximal region of the epididymis, spermatozoa do not undergo maturation, resulting in male infertility. The tumor suppressor phosphatase and tensin homolog (PTEN) was deleted from the initial segment, which resulted in changes in the activity of downstream signaling components that led to epithelial dedifferentiation and male infertility. Spermatozoa were normal upon leaving the testis, but as they progressed through the duct of the dedifferentiated initial segment, they developed angled flagella and a decrease in motility. These changes prevented spermatozoa from reaching and fertilizing an egg in the female reproductive tract. PTEN plays an essential role in maintaining normal initial-segment differentiation and function and, therefore, male fertility.

Author contributions: B.X. and B.T.H. designed research; B.X. and A.M.W. performed research; B.X. and B.T.H. analyzed data; and B.X. and B.T.H. wrote the paper.

The authors declare no conflict of interest.

This article is a PNAS Direct Submission.

[1]To whom correspondence should be addressed. Email: bth7c@virginia.edu.

This article contains supporting information online at www.pnas.org/lookup/suppl/doi:10.1073/pnas.1413186112/-/DCSupplemental.

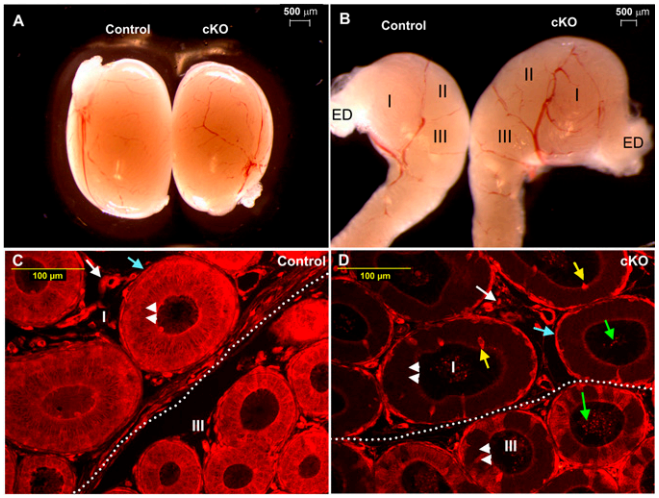

Fig. 1. Hypertrophy of the proximal epididymis at P28 shortly after *Pten* deletion. (*A*) Testes from control and cKO animals. (*B*) Proximal epididymal regions (I, II, and III) from control and cKO animals. (*C*) Immunofluorescence (IF) of PTEN in control epididymal regions I and III. (*D*) IF of PTEN in cKO epididymal regions I and III. The dotted line shows the border between regions I and III. Double arrowheads label epithelial cells; light blue arrows label mesenchymal cells; white arrows label cells in the interstices; green arrows label spermatozoa; yellow arrows labels narrow cells. ED, efferent ducts.

evident in proximal epididymal regions I, II, and III in conditional knockout (cKO) animals (Fig. 1*B*), whereas testicular size of cKOs and their littermate controls did not display differences (Fig. 1*A*).

Immunofluorescent analysis showed that PTEN had ubiquitous expression in epithelial cells, surrounding mesenchymal cells, and interstitial cells in controls (Fig. 1*C*). However, in cKOs, PTEN expression was absent from most epithelial cells in region I, except for narrow cells (Fig. 1*D,* yellow arrows), and PTEN displayed a mosaic expression in region III epithelium (Fig. 1*D*). In addition, PTEN remained in mesenchymal cells, interstitial cells, and spermatozoa in cKO regions I and III (Fig. 1*D*). The pattern of PTEN deletion in our cKOs was consistent with reported expression patterns of *Rnase10*–Cre (9, 10). Fig. S1 illustrates initial-segment regions I, II, and caput region III, which were defined according to previous studies (11, 12). Fig. S2 shows low autofluorescence of the epididymis and low background of secondary antibody labeling alone in our immunofluorescent experiments.

Changes in the Activity Levels of the AKT and ERK Pathway Components Shortly After *Pten* Deletion. At P28, shortly after *Pten* deletion, PTEN protein level declined in cKO regions I and II compared with similar control regions (Fig. 2*A*). The remaining PTEN expression in cKOs was presumably from mesenchymal cells, interstitial cells, and spermatozoa because PTEN was only removed from the epithelium and was still present in other cell types (Fig. 1*D*).

Consistent with decreased PTEN protein level, several AKT pathway components showed significant increases in their activity levels at P28 after loss of *Pten* (Fig. 2*A*). The phosphorylation levels of AKT at S473, RPS6 at S235/S236, and GSK3A/B at S21/S9 increased in cKO regions I and II compared with controls. The phosphorylation levels of MTOR at S2448 showed a slight increase in region I. Androgen receptor (AR) protein level did not change significantly (Fig. 2*A*).

Furthermore, down-regulation of the activity levels of the ERK pathway components became apparent at P28 in cKOs (Fig. 2*B*). Although the phosphorylation level of RAF1 at the activation site S338 did not change, the phosphorylation level of RAF1 at S259, an inhibitory site targeted by AKT (13), increased in cKO regions I and II. The phosphorylation levels of MAPK3/1 at T202/Y204 declined in region II but remained high in region I after loss of *Pten*. However, the MAPK1 protein level did not change significantly. At P28, the protein level of ETS variant gene 4 (ETV4), a downstream gene of the ERK pathway, declined in cKO regions I and II compared with controls (Fig. 2*B*).

Immunofluorescent analysis confirmed our Western results of activation of the AKT pathway components after loss of *Pten* (Fig. S3). At P28, the phosphorylation levels of ATK/MTOR/RPS6/GSK3 at their activation sites increased in cKO region I compared with controls (Fig. S3). Unchanged or slightly changed labeling intensity of these proteins in region III served as controls to highlight the initial-segment–specific activation (Fig. S3).

In addition, immunofluorescent analysis confirmed declined activity levels of the ERK pathway components in cKO region II at P28 (Fig. S4). Compared with controls, the phosphorylation level of RAF1 at its inhibitory site S259 increased, whereas the phosphorylation levels of MAP2K1/2 and MAPK3/1 at their activation sites decreased in cKO region II. In contrast to region II, changes in activity levels of these kinases in region I were undetectable at P28 shortly after *Pten* deletion (Fig. S4).

Progressive Decline of MAPK3/1 Activities in the Initial Segment After Loss of *Pten*. The low-magnification images in Fig. 3 show immunofluorescent labeling of phospho-MAPK3/1 in the sections cut through the center of the proximal epididymides along the epididymal axis. As expected, the control initial segments at 4 wk and 6 and 12 mo displayed higher phospho-MAPK3/1 levels (Fig. 3 *A*, *C*, and *E*). The intensity of phospho-MAPK3/1 labeling gradually declined in the control initial segment from proximal to distal (Fig. 3 *A*, *C*, and *E*). In cKOs, phospho-MAPK3/1 levels declined in region II at 4 wk (Fig. 3*B*) and declined further to most of region I at 6 mo (Fig. 3*D*). Only a small area of region I, which is closest to the efferent ducts, displayed elevated phospho-MAPK3/1 levels at 6 mo (Fig. 3*D*). The intensity of the elevated phospho-MAPK3/1 levels in that small area of cKOs was also lower compared with controls at 12 mo (Fig. 3*F*).

Changes of Two Major Initial-Segment Cell Types After Loss of *Pten*. Changes of two major types of epithelial cells, principal and basal cells, were observed in the cKO epithelium at P28. As shown in Fig. 4, KRT5 was present intracellularly in basal cells, which outlined their shape. The control initial segment had triangle-

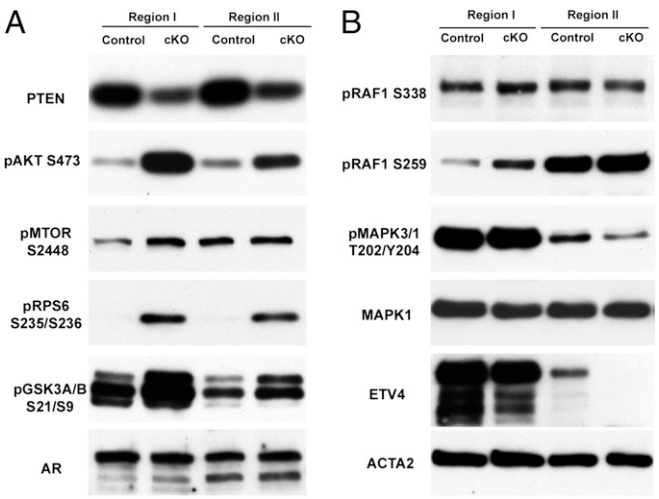

Fig. 2. Western blot analysis of protein and/or phosphorylation levels of the AKT and ERK pathway components at P28. (*A*) Protein levels of PTEN and AR and phosphorylation levels of the AKT pathway components, AKT/MTOR/RPS6/GSK3, in control and cKO regions I and II. (*B*) Phosphorylation levels of RAF1 and MAPK3/1 and protein levels of MAPK1 and ETV4 in control and cKO regions I and II. ACTA2 served as a loading control.

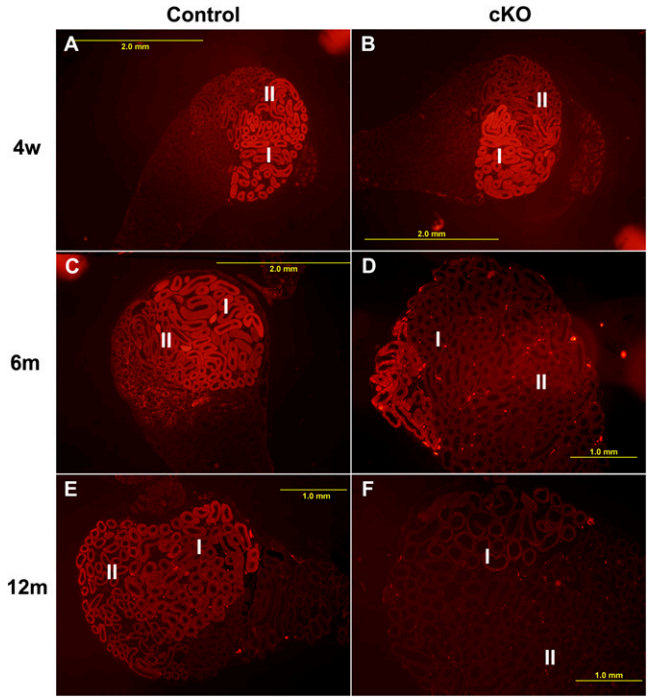

Fig. 3. Progressive decrease in the activity levels of MAPK3/1 in regions I and II after loss of *Pten*. (*A*, *C*, and *E*) phospho-MAPK3/1 levels in the control initial segments at ages 4 wk, 6 mo, and 12 mo. (*B*, *D*, and *F*) phospho-MAPK3/1 levels in the cKO initial segments at ages 4 wk, 6 mo, and 12 mo.

shaped basal cells with long projections toward the lumen (Fig. 4 *A* and *C*). Compared with controls, cKO basal cells had shortened projections (Fig. 4 *B* and *D*), especially in region II (Fig. 4*D*). ETV4 labeled the nuclei of principal cells in control regions I and II (Fig. 4 *E* and *G*), but labeling was reduced in cKO region I (Fig. 4*F*) and was undetectable in cKO region II (Fig. 4*H*). In addition, CDH2 labeled the basal–lateral membrane and outlined the shape of all types of epithelial cells. At P28, the control initial segment had tall, columnar principal cells (Fig. 4 *I* and *K*), whereas principal cells in cKOs were rounder or atypically shaped (Fig. 4 *J* and *L*). Their height was shorter compared with controls at ages 10 wk, 6 mo, and 12 mo (Fig. 5*G*).

Progressive Changes in Cell Shape, Size, and Organization of the Initial-Segment Epithelium After Loss of *Pten*. The morphological changes after loss of *Pten* were evident at P28. Subtle changes, such as curvature of the epithelial apical surface, were observed in cKO region I (Fig. S5*B*), but a few areas in region II showed changes in cell shape, size, and organization, which resulted in epithelial folding (Fig. S5*D*). At 10 wk, cKO regions I and II demonstrated extensive epithelial folding (Fig. 5*D* and Fig. S5 *F* and *H*). Protrusion of the epithelium into the lumen, due to folding, resulted in blockage of spermatozoa progression in 11.7% ($n = 34$) epididymides collected from cKO mice older than 10 wk. However, blockage was not found in littermate controls ($n = 36$). At 6 mo, epithelial cells not only protruded toward the lumen, but also toward the basement membrane (Fig. 5*F*).

Compared with controls, the epithelium of cKO region I had significantly reduced height at ages 10 wk, 6 mo, and 12 mo (Fig. 5*G*) and had increased area with atypically shaped epithelial cells from 10 wk onward (Fig. 5*H*). From 10 wk onward, epithelial cell size increased in cKOs, which presumably contributed to a hypertrophy phenotype (Fig. 5*I*).

Tight Junction and Basement Membrane Integrity Following Loss of *Pten*. Both phospho-APKC (atypical PKC) and TJP1 labeled the intact ring structure of tight junctions at the apical region of the epithelium in 6-mo-old controls and cKOs (Fig. S6 *A–D*). COL4 labeled the intact basement membrane surrounding epithelial cells in 6-mo-old controls and cKOs (Fig. S6 *E* and *F*).

Changes in Proliferation and Apoptosis After Loss of *Pten* for Longer Periods of Time. Although a hypertrophy phenotype was observed as early as 4 wk, proliferation in the epithelium of cKOs was similar to controls at 4 and 10 wk. From 16 wk onward, proliferation increased moderately but significantly in the cKO epithelium compared with controls (Fig. S7*A*). Moreover, at 4 and 10 wk, apoptosis in cKO epithelial cells was not significantly different compared with controls. However, there was a moderate but significant increase of apoptosis in the epithelium of cKOs compared with controls from 16 wk onward (Fig. S7*B*).

Progressive Loss of Male Fertility After Loss of *Pten*. To test fertility, a group of cKO and littermate control males was each mated with wild-type females. All of the tested controls were fertile from ages 3–12 mo. The cKO males were fertile from ages 3–5 mo but progressively lost fertility from age 6 mo onward. At age 7 mo, 67% of cKO males were already infertile, whereas 33% of them were subfertile and sired significantly fewer numbers of litters

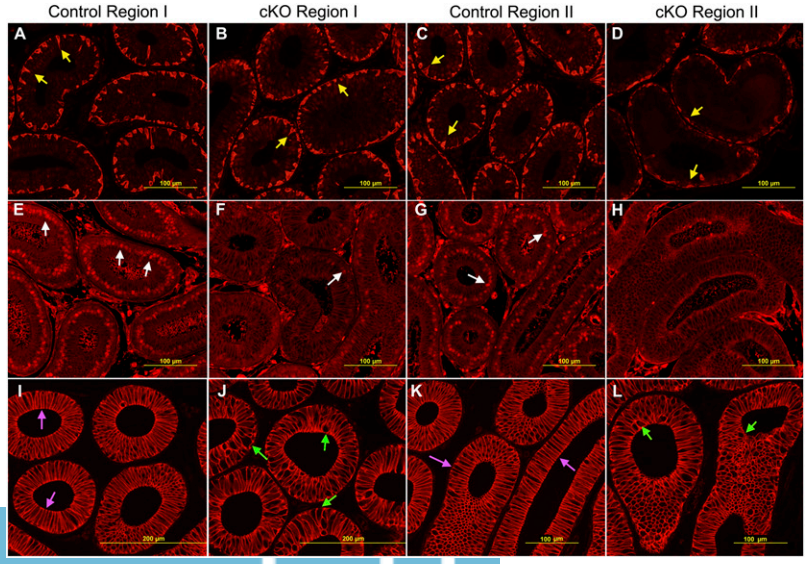

Fig. 4. Identification of principal and basal cells in control and cKO epididymal epithelium at P28. (*A–D*) Comparison of KRT5-labeled basal cells between controls and cKOs in regions I and II. (*E–H*) Comparison of ETV4 labeling at principal cells nuclei between controls and cKOs in regions I and II. (*I–L*) Comparison of CDH2-labeled epithelial cells between controls and cKOs in regions I and II. Yellow arrows label the projections of basal cells; white arrows indicate the nuclear labeling of ETV4; magenta arrows label tall, columnar principal cells; green arrows label atypically shaped epithelial cells including spherical, oval, and irregular-shaped cells.

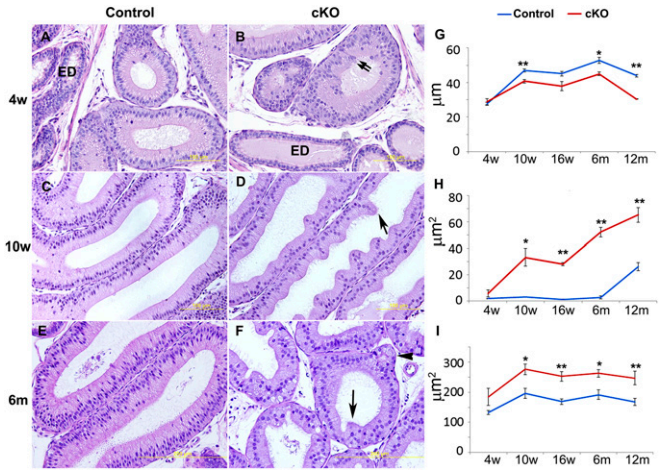

Fig. 5. Progressive morphological changes in the cKO initial-segment epithelium. (*A*, *C*, and *E*) Representative images of control region I at age 4 wk, 10 wk, and 6 mo. (*B*, *D*, and *F*) Representative images of cKO region I at age 4 wk, 10 wk, and 6 mo. Double arrows label a disorganized epithelial region; single arrows label protrusion of epithelial cells toward the lumen; and an arrowhead labels a protrusion toward the basement membrane. ED, efferent ducts. (*G*) Comparison of epithelial height between cKOs and controls in region I over a year. (*H*) Comparison of the epithelial area with atypically shaped cells between cKOs and controls in region I over a year. (*I*) Comparison of the size of epithelial cells between cKOs and controls in region I over a year. Data are represented as mean ± SEM. $*P < 0.05$; $**P < 0.01$.

compared with controls. All cKO males became infertile at age 12 mo (Fig. 6). Although the average number of litters sired by cKO males from age 3–6 mo were not significantly different compared with controls, the average litter size of cKOs in this age group was already significantly lower compared with controls ($P < 0.05$) (Table S1). Moreover, the few subfertile cKO males from age 7–12 mo sired significantly fewer numbers of litters compared with controls ($P < 0.01$). The very few litters sired by the cKO males of this age group only had one or two pups in each litter (Table S1). To investigate whether the infertile phenotype was due to abnormal mating behavior, the frequency of presence of vaginal plug was examined from the ages of 9–10 mo. The plug frequency did not show significant differences between cKOs (3.5 ± 0.5 d per plug; mean ± SEM) and controls (4.2 ± 0.4 d per plug), indicating that older cKO males still mated normally, similar to littermate controls. The infertility caused by blockage of epididymides was excluded from Fig. 6 and Table S1.

Spermatozoa Flagellar Angulation and Declined Spermatozoa Motility After Loss of *Pten*. A progressive decline in spermatozoa motility coupled with an increase in flagellar angulation from 10 wk to 12 mo in cKOs was observed (Fig. 7 *A* and *B*). Cauda spermatozoa from 10-wk-old cKOs had normal motility and low percentage of flagellar angulation. At 16 wk, one of four epididymides showed a high percentage of flagellar angulation and low motility, but the average was not significantly different compared with controls. From 6 mo onward, cauda spermatozoa from cKOs had significant lower motility and higher percentage of flagellar angulation compared with controls (Fig. 7 *A* and *B*).

Despite normal testis weight and cauda spermatozoa count in 6-mo-old cKOs (103 ± 2 mg; $5.32 \pm 1.39 \times 10^7$ spermatozoa; mean ± SEM) and controls (97 ± 2 mg; $5.69 \pm 0.59 \times 10^7$ spermatozoa), spermatozoa from cKOs showed maturation defects after progression through the epididymis at age 6 mo (Fig. 7 *C*–*G*). First, in situ spermatozoa from fixed tissues (Fig. 7*C*) were analyzed. Spermatozoa were straight in the testis and initial segment. However, cauda spermatozoa had increased flagellar angulation in cKOs compared with controls, suggesting that flagellar angulation occurred during epididymal transit. Furthermore, spermatozoa from different regions of the male tract behaved differently when released into Biggers–Whitten–Whittingham (BWW) medium. In controls, testicular and initial-segment spermatozoa were straight but immotile; caput spermatozoa were motile but displayed flagellar angulation and moved in a circular, nonprogressive motion; corpus and cauda spermatozoa gained normal motility and ability to maintain straight flagella (Fig. 7 *D* and *E*). In cKOs, spermatozoa from the testis and initial segment appeared normal, but never fully gained maturation characteristics during epididymal transit. cKO corpus and cauda spermatozoa still displayed low motility and flagellar angulation similar to normal caput spermatozoa (Fig. 7 *D* and *E*). High percentages of motile spermatozoa from the caput, corpus, and cauda were angled in cKOs (Fig. 7*F*) and did not progress normally. Consistently, computer-assisted semen analysis (CASA) of spermatozoa kinematics revealed a significant decline in curvilinear velocity (VCL) of cKO cauda motile spermatozoa compared with controls (Fig. 7*G*).

The morphology of cKO testes was similar to control testis at age 12 mo (Fig. S8). However, cauda spermatozoa from 12-mo-old cKOs displayed severe defects (Fig. S9). Unlike controls (Movie S1), the majority of cKO spermatozoa displayed in situ flagellar angulation, which included hairpin (complete 180° bending at the localization of the cytoplasmic droplet; Movie S2) and half-hairpin (<180° but ≥90° bending; Movie S2). Hairpin angulation was the dominant form among angled cKO spermatozoa. When spermatozoa were incubated in BWW medium, a high percentage of cKO spermatozoa were angled (Fig. S9*B*), and a low percentage of them were motile (Fig. S9*C*). Among motile cKO spermatozoa, approximately half were angled (Fig. S9*D*). Consistent with the observation that angled spermatozoa did not progress normally as straight spermatozoa (Movies S1 and S2), VCL of cKO motile spermatozoa was lower compared with controls (Fig. S9*E*). The duration of incubation did not affect spermatozoa behavior (Fig. S9 *B*–*E*).

***Ros1* Expression After Loss of *Pten*.** To determine whether PTEN signals through ROS1—an essential signaling molecule for initial-segment–prepubertal differentiation—*Ros1* mRNA level in the initial segment of 6-mo-old *Pten* cKOs was analyzed (Fig. S10). *Ros1* mRNA level did not change significantly after loss of *Pten*, whereas the mRNA level of *Etv4*, a downstream gene of MAPK3/1, decreased to approximately 1/10 of the control level, and the *Ar* mRNA level did not change (Fig. S10).

Discussion

Regulation of the ERK and AKT pathways are important for cell survival, proliferation, metabolism, and motility (14). Our previous studies demonstrated that the high activity levels of the ERK pathway components were essential for differentiation of the initial-segment epithelium (5, 8). However, the role of the AKT pathway in the development of the initial segment is unclear, although the high expression and activity levels of PTEN are a unique feature of a differentiated initial segment (5). In this study, we conditionally removed *Pten* from the epithelial

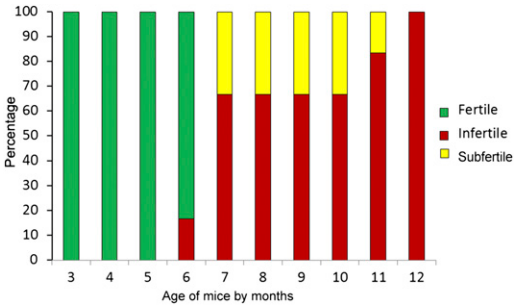

Fig. 6. Progressive loss of fertility in cKO mice. Percentages of fertile (green), subfertile (yellow), and infertile (red) cKO male mice from 3 to 12 mo are shown.

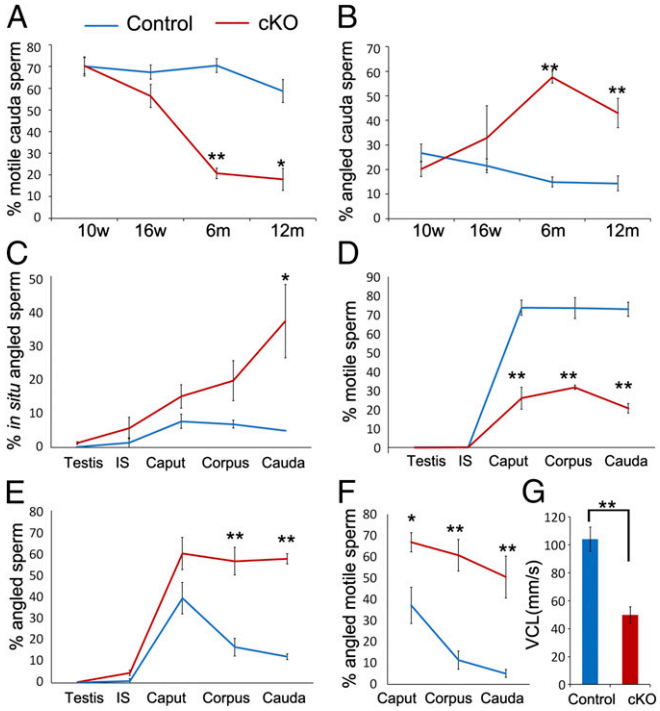

Fig. 7. Comparison of spermatozoa motility and flagellar angulation between cKOs and controls. (*A*) Comparison of spermatozoa motility between cKOs and controls over a year. (*B*) Comparison of flagellar angulation between cKOs and controls over a year. (*C*) Percentages of in situ spermatozoa with flagellar angulation in the testis and epididymal regions at age 6 mo. (*D*) Percentages of motile spermatozoa from the testis and epididymal regions at age 6 mo. (*E*) Percentages of spermatozoa with flagellar angulation from the testis and epididymal regions at age 6 mo. (*F*) Percentages of motile spermatozoa with flagellar angulation from the caput, corpus, and cauda at age 6 mo. (*G*) VCL of motile spermatozoa from the cauda of controls and cKOs at age 6 mo. $*P < 0.05$; $**P < 0.01$.

cells of the initial segment, which resulted in the activation of the AKT pathway components that, in turn, suppressed the activity levels of the ERK pathway components. The altered pathways resulted in a series of morphological changes that reflected initial-segment epithelial dedifferentation. The dedifferentiated initial segment eventually led to male infertility due to compromised sperm maturation. Therefore, both high activity levels of the ERK pathway components and low activity levels of the AKT pathway components are critical for a normal functioning initial segment. The knockout phenotype was probably not due to secondary/indirect factors such as changes in androgen levels because spermatogenesis, testicular weights, cauda spermatozoa counts, AR expression, and mating behavior observed in these mice were similar to controls. Furthermore, the males and females of the two genetically modified mouse lines, *Rnase10*–Cre and floxed–*Pten*, were healthy, viable, and fertile, suggesting that any secondary/indirect factors originating from each animal line affecting the phenotype of initial-segment–specific *Pten* knockout were minimal.

There is substantial evidence for cross-talk between the ERK and AKT pathways (14)—either positively by cross-activation or negatively by cross-inhibition, depending upon the cellular environment (14). In this study, the cross-talk between the ERK and AKT pathways in the initial segment was observed through the interaction of AKT and RAF1. Both Western blot and immunofluorescent data showed increased phosphorylation level of RAF1 at S259 after AKT activation. Most interestingly, the suppression of the ERK pathway in this study was progressive. Because *Rnase10*-mediated *Pten* deletion began at P17, the ERK pathway was already activated in the knockout initial segment. The suppression of MAPK3/1 activities, caused by *Pten* deletion, gradually extended from region II to region I (Fig. 3). This observation may imply that other inputs/resources, likely testicular luminal fluid factors, countered such suppression. Fig. 3 shows that the activity levels of MAPK3/1 gradually declined in the control initial segment from proximal to distal. Presumably, such a gradient resulted from the gradual decline in concentration of testicular luminal factors along the epididymal duct. The AKT pathway, activated by loss of *Pten,* initially suppressed the lower activity levels of MAPK3/1 in region II, but at later times, suppressed the higher activity level in region I. This finding may explain why changes in activities of several signaling molecules and changes in epithelial morphology occurred from region II to region I over time.

Loss of *Pten* altered cell shape, size, and organization in the initial segment. Cell shape is commonly used as a marker to reflect cell differentiation. Dysregulation of AKT signaling due to PTEN deficiency caused cells to dedifferentiate in several tissues (15, 16). Initial-segment differentiation is commonly characterized by tall, columnar principal cells (6) and triangular basal cells with long projections (7). In initial-segment–specific *Pten* knockout, principal cells were shorter and irregular, and basal cells had shortened projections (Fig. 4), suggesting dedifferentiation. Cell-size changes have accounted for hypertrophy phenotypes observed in multiple tissue-specific *Pten* knockout models (17). Several downstream molecules of the AKT pathway—including PRS6KB1, MTOR, EIF4EBP1, and RPS6—were involved in the control of protein synthesis and were shown to be regulators of cell size (17). In this study, we observed increased activities of MTOR and RPS6 and increased cell size after *Pten* deletion. These findings provide further evidence that cell size is regulated by PTEN and its downstream components. The most pronounced change in cellular organization in initial-segment–specific *Pten* knockouts was extensive epithelial folding. In the male reproductive tract, epithelial folding has only been observed in mouse efferent ducts after constitutive activation of NOTCH1 signaling (18) and has not been observed in other *Pten* knockout models. During normal tissue morphogenesis, epithelial folding is mediated by cell shape changes driven by apical constriction or, alternatively, by differential positioning of adherens junctions (19). Whether this process occurs in the initial segment after loss of *Pten* is unclear, but our data suggest that PTEN is a regulator of epithelial folding.

PTEN regulates cell proliferation in a tissue-dependent manner. Aberration of AKT signaling resulted in hyperproliferation and hyperplasia in most PTEN-deficient tissues, with a few exceptions (15, 17, 20). PTEN is probably not a major regulator of cell proliferation in the initial segment because loss of *Pten* did not alter proliferation in younger knockout mice and only resulted in a moderate increase in cell proliferation from 16 wk onward. In tissue-specific *Pten* knockout animals, loss of *Pten* led to cancer development in some animals, but not in others (21, 22). For those tissues in which cancer was not observed, additional molecular events were needed to overturn the regulatory machinery of cell proliferation and survival (15). Cancer development was not observed in initial segments after loss of *Pten* despite some being twice the size of controls. It is not clear why the epididymis rarely succumbs to cancer (23). Here, we demonstrated cross-inhibition between the AKT and ERK pathways in the initial segment. Hypothetically, if the cross-inhibition were dominant in the interaction between the two pathways, it would be difficult for both proproliferative pathways to be activated aberrantly. Further studies are needed to determine whether this hypothesis is one of the reasons that the epididymis rarely develops cancer. Interestingly, cross-activation of the same two pathways was often observed in cancer malignancies in other tissues (14, 24).

We observed elevated apoptosis after the activation of the AKT pathway by loss of *Pten*, in contrast to other tissues in which the AKT pathway is normally considered to be an antiapoptotic pathway (15). Our findings are probably the result of a secondary effect of disorganization of epithelial cells after *Pten* deletion. In particular, a moderate increase in apoptosis was observed only

after knockout epithelial cells underwent substantial changes. Most importantly, although loss of *Pten* caused substantial changes in the epithelium, tight junction integrity and apical–basal polarity in the knockout initial segment remained. Additionally, in knockouts, protrusion of epithelial cells toward the basement membrane did not affect the integrity of the basement membrane.

Spermatozoa flagellar angulation was phenotypically associated with dysfunction of the initial segment in initial-segment–specific *Pten* knockouts. A similar phenotype was also observed in two other animal models: *Ros1* knockouts (3) and glutathione peroxidase 5 (*Gpx5*)–TAG2 transgenic mice, the latter of which expressed Simian virus 40 small T-antigen driven by *Gpx5* promoter (25). The histological changes of the initial segment of all three models were similar but not identical. In *Ros1* knockouts, the epithelium failed to undergo prepubertal differentiation (3), whereas the epithelium of *Gpx5*–TAG2 mice was slightly hyperplastic (25). In the present study, epithelial hypertrophy was observed.

Although the histological appearance of the initial segment was different in each animal model, a defect in differentiation could be a common underlining mechanism of loss-of-function of the initial segment. First, it was clear that *Ros1* knockouts lacked a differentiated initial segment (3). Second, lack of expression of several genes specific for the initial segment in *Gpx5*–TAG2 mice suggested an arrest of initial-segment differentiation (25). Third, in initial-segment–specific *Pten* knockouts, high MAPK3/1 activity levels and high ETV4 protein level in the initial segment—which are the markers of initial-segment differentiation (5, 26)—gradually diminished after *Pten* deletion (Figs. 3 and 4). Furthermore, epithelial height and the shape of principal and basal cells, which are often used to identify initial-segment differentiation (6), changed after *Pten* deletion (Figs. 4 and 5). These lines of evidence suggested dedifferentiation of the initial segment in initial-segment–specific *Pten* knockouts. Loss of differentiation of the initial segment would presumably lead to a failure of this epithelium to generate a normal luminal microenvironment necessary for sperm maturation, as shown in the *Ros1* knockout (3, 4, 27, 28).

A common feature of spermatozoa in these three models was an increase in flagellar angulation (4, 25, 27). In wild types, testicular and initial-segment spermatozoa were straight, but immotile. Caput spermatozoa were motile, but displayed flagellar angulation and moved in a circular nonprogressive motion when challenged with hypotonic medium, which mimics the osmolarity of fluid from the female tract (28). When normal corpus and cauda spermatozoa encountered the same hypotonic medium, they triggered a regulatory volume decrease to maintain straight flagella (28). By contrast, knockout spermatozoa from the three models exhibited flagellar angulation after hypotonic challenge and also displayed an increase in flagellar angulation as they progressed along the epididymal duct. The spermatozoa phenotype was more severe in initial-segment–specific *Pten* knockouts and *Gpx5*–TAG2 mice because hairpin was the major angulation form in these two models, whereas half-hairpin was the dominant form in *Ros1* knockouts.

Despite the similar phenotype in *Ros1* and initial-segment–specific *Pten* knockouts, *Pten* deletion did not affect *Ros1* mRNA expression. Therefore, PTEN signaling is likely independent of ROS1 signaling. Because both PTEN and ROS1 (29) are upstream regulators of ERK signaling, it is possible that PTEN and ROS1 signaling are independent but converge to regulate ERK signaling, which, in turn, regulates differentiation of the initial segment.

In summary, under normal physiological conditions, PTEN signals through RAF1/ERK to maintain normal function of the initial segment and male fertility.

Materials and Methods

Materials and procedures are described in *SI Materials and Methods*, including details of mice lines, Western blots, immunofluorescence, real-time PCR, measurement of cell proliferation and apoptosis, mating and assessment of male fertility, and measurement of spermatozoa motility, flagellar angulation, and kinematic parameters.

ACKNOWLEDGMENTS. We thank Yuesheng Li, Akwasi Asante, and Hameeda Naimi for assistance in performing experiments and reviewing the manuscript; and Maria Teves for assistance with sperm analysis. This work was supported by Eunice Kennedy Shriver National Institute of Child Health and Human Development/NIH Grant R01 HD068365.

1. Hinton BT, et al. (2011) How do you get six meters of epididymis inside a human scrotum? *J Androl* 32(6):558–564.
2. Robaire B, Hinton B, Orgebin-Crist M (2006) The epididymis. *Knobil and Neill's Physiology of Reproduction*, ed Neill J (Elsevier, New York), 3 Ed, pp 1071–1148.
3. Sonnenberg-Riethmacher E, Walter B, Riethmacher D, Gödecke S, Birchmeier C (1996) The c-ros tyrosine kinase receptor controls regionalization and differentiation of epithelial cells in the epididymis. *Genes Dev* 10(10):1184–1193.
4. Yeung CH, Sonnenberg-Riethmacher E, Cooper TG (1999) Infertile spermatozoa of c-ros tyrosine kinase receptor knockout mice show flagellar angulation and maturational defects in cell volume regulatory mechanisms. *Biol Reprod* 61(4):1062–1069.
5. Xu B, Yang L, Lye RJ, Hinton BT (2010) p-MAPK1/3 and DUSP6 regulate epididymal cell proliferation and survival in a region-specific manner in mice. *Biol Reprod* 83(5):807–817.
6. Rodriguez C, Kirby J, Hinton B (2002) The development of the epididymis. *The Epididymis: From Molecules to Clinical Practice*, eds Robaire B, Hinton B (Kluwer Academic/Plenum, New York), pp 251–267.
7. Shum WW, et al. (2008) Transepithelial projections from basal cells are luminal sensors in pseudostratified epithelia. *Cell* 135(6):1108–1117.
8. Xu B, et al. (2011) Testicular lumicrine factors regulate ERK, STAT, and NFKB pathways in the initial segment of the rat epididymis to prevent apoptosis. *Biol Reprod* 84(6):1282–1291.
9. Krutskikh A, et al. (2011) Targeted inactivation of the androgen receptor gene in murine proximal epididymis causes epithelial hypotrophy and obstructive azoospermia. *Endocrinology* 152(2):689–696.
10. Xu B, Yang L, Hinton BT (2013) The Role of fibroblast growth factor receptor substrate 2 (FRS2) in the regulation of two activity levels of the components of the extracellular signal-regulated kinase (ERK) pathway in the mouse epididymis. *Biol Reprod* 89(2):1–13.
11. Jelinsky SA, et al. (2007) The rat epididymal transcriptome: Comparison of segmental gene expression in the rat and mouse epididymides. *Biol Reprod* 76(4):561–570.
12. Robaire B, Hermo L (1988) Efferent duct, epididymis, and vas deferens: Structure, functions, and their regulation. *The physiology of reproduction*, eds Knobil E, Neill J (Raven Press, New York), Vol 1, pp 999–1080.
13. Zimmermann S, Moelling K (1999) Phosphorylation and regulation of Raf by Akt (protein kinase B). *Science* 286(5445):1741–1744.
14. Mendoza MC, Er EE, Blenis J (2011) The Ras-ERK and PI3K-mTOR pathways: Cross-talk and compensation. *Trends Biochem Sci* 36(6):320–328.
15. Knobbe CB, Lapin V, Suzuki A, Mak TW (2008) The roles of PTEN in development, physiology and tumorigenesis in mouse models: A tissue-by-tissue survey. *Oncogene* 27(41):5398–5415.
16. Furgeson SB, et al. (2010) Inactivation of the tumour suppressor, PTEN, in smooth muscle promotes a pro-inflammatory phenotype and enhances neointima formation. *Cardiovasc Res* 86(2):274–282.
17. Backman S, Stambolic V, Mak T (2002) PTEN function in mammalian cell size regulation. *Curr Opin Neurobiol* 12(5):516–522.
18. Lupien M, et al. (2006) Expression of constitutively active Notch1 in male genital tracts results in ectopic growth and blockage of efferent ducts, epididymal hyperplasia and sterility. *Dev Biol* 300(2):497–511.
19. Wang YC, Khan Z, Kaschube M, Wieschaus EF (2012) Differential positioning of adherens junctions is associated with initiation of epithelial folding. *Nature* 484(7394):390–393.
20. Yoo LI, et al. (2006) Pten deficiency activates distinct downstream signaling pathways in a tissue-specific manner. *Cancer Res* 66(4):1929–1939.
21. Backman SA, et al. (2004) Early onset of neoplasia in the prostate and skin of mice with tissue-specific deletion of Pten. *Proc Natl Acad Sci USA* 101(6):1725–1730.
22. Hernando E, et al. (2007) The AKT-mTOR pathway plays a critical role in the development of leiomyosarcomas. *Nat Med* 13(6):748–753.
23. Okazaki IJ, Pryor JL (2002) Cancer of the epididymis. *The Epididymis: From Molecules to Clinical Practice*, eds Robaire B, Hinton BT (Kluwer Academic/Plenum, New York), pp 555–561.
24. Chetram MA, Hinton CV (2012) PTEN regulation of ERK1/2 signaling in cancer. *J Recept Signal Transduct Res* 32(4):190–195.
25. Sipilä P, et al. (2002) Epididymal dysfunction initiated by the expression of simian virus 40 T-antigen leads to angulated sperm flagella and infertility in transgenic mice. *Mol Endocrinol* 16(11):2603–2617.
26. Yang L, Fox SA, Kirby JL, Troan BV, Hinton BT (2006) Putative regulation of expression of members of the Ets variant 4 transcription factor family and their downstream targets in the rat epididymis. *Biol Reprod* 74(4):714–720.
27. Cooper TG, et al. (2004) Mouse models of infertility due to swollen spermatozoa. *Mol Cell Endocrinol* 216(1-2):55–63.
28. Yeung CH, et al. (2002) Sperm volume regulation: Maturational changes in fertile and infertile transgenic mice and association with kinematics and tail angulation. *Biol Reprod* 67(1):269–275.
29. Jun HJ, et al. (2014) ROS1 signaling regulates epithelial differentiation in the epididymis. *Endocrinology* 155(9):3661–3673.